Journal of Visualization, Vol. 7, No. 4 (2004) 317-329

Simulation of Winter Air Pollution Dispersion Mechanism of Kathmandu Valley by Water-Tank Experiment

Shrestha, M. L.[*1], Kaga, A.[*1], Kondo, A.[*1], Inoue, Y.[*1], Sugisawa, M.[*1] and Sapkota, B.[*2]

*1 Department of Environmental Engineering, Osaka University, 2-1, Yamada-Oka, Suita, Osaka 565-0871, Japan. Tel: +81-6-6879-7670 / FAX: +81-6-6879-7669
E-mail: manohar@moon.env.eng.osaka-u.ac.jp
*2 Institute of Engineering, Pulchowk Campus, Tribhuvan University, Lalitpur, Nepal.

Received 11 February 2004
Revised 11 July 2004

***Abstract*:** The air pollution concentration in Kathmandu valley in the winter season was found to be higher than in the summer season due to the formation of the inversion layer. This mechanism was simulated in the water-tank experiment by measuring the temperature and flow field using liquid crystal thermometry and particle image velocimetry. Thermal stratification was made at the beginning of the experiment and the surface temperature of the valley model was changed with 12 minutes period matching the diurnal field temperature pattern of the Kathmandu valley. The updraft wind and Bernard convection occurred during daytime and downdraft wind and inversion layer were realized during nighttime. The temperature, flow field and mass dispersion characteristics obtained in the water-tank experiment explained clearly the mechanism of air pollution in Kathmandu valley.

***Keywords*:** Kathmandu Valley, Water-Tank Experiment, Inversion Layer, Flow Field, PIV.

1. Introduction

Kathmandu, the Capital of Nepal, has an altitude of approximately 1400 m above the sea level and is surrounded by many mountains having about 1000 m height from the ground level of the valley. Due to the bowl-shaped topographical structure of Kathmandu valley, the air circulation in the valley is very weak and easy to trap the pollution emitted inside the valley. The atmospheric pollution in Kathmandu is getting worse and is found to be higher during winter season. The authors measured the concentration of NO_2, total suspended particulate (TSP) and temperature in Kathmandu during winter season in 2001. It was found that the concentration of NO_2 and TSP became high in the morning and a strong inversion layer was formed from midnight to early morning (Shrestha et al., 2001). The formation of inversion layer was verified by the vertical height temperature measurement in Kathmandu valley (Shrestha et al., 2002a; Kondo et al., 2002). The vertical distribution of the meteorological and pollutants data helps to understand the pollution dispersion mechanism in the valley but such data are not available in Kathmandu yet. The understanding of pollution dispersion mechanism in the Kathmandu valley helps to make counter measurement policy regarding the air pollutant in Kathmandu valley.

The purpose of this research is to find out the air pollution dispersion mechanism over Kathmandu during the winter season by performing a water-tank experiment. Although wind tunnel experiments are carried out for an atmospheric air pollution, generally it is very difficult to understand air pollution phenomenon caused by natural convection in a wind tunnel because of high

turbulence of air and difficulty to obtain stable layer of air above the ground surface. Therefore, the water-tank experiment which can realize similar winter atmospheric condition was chosen. The water-tank experiments that simulate the atmospheric phenomena caused by natural convection were done by several researchers. Matsumoto and Ueda (1983) and Kaga et al. (1995) simulated the land and sea breeze circulation in a laboratory using a temperature controlled water-tank. Heping et al. (2001) simulated the plume dispersion in stratified atmosphere of Hong Kong Island. Ohba et al. (1991) studied the plume rise and diffusion of gases discharged from a stack under calm and unstable condition using a water tank. Park et al. (2001) compared mesoscale measurement of vertical dispersion coefficient by using a composite turbulence water tank and convective diffusion observed with remote sensors field data. All these researchers suggested the atmospheric phenomenon and pollutant dispersion qualitatively by applying water-tank experiments. In our study, quantitative analysis of visualization techniques was used as a tool of experiment to measure and verify the vertical atmospheric phenomenon near the ground surface of Kathmandu valley creating the winter atmospheric stable layer in the water-tank experiment.

2. Water-Tank Experiment

2.1 Similarity Rule

The experiment was carried out by using the dimensionless variable proposed by Ueda (1983). The proposed dimensionless variables of wind speed, horizontal length and vertical length shown in equation 1, 2 and 3, respectively, may be the universal similarity variables for comparing field measurements with laboratory-scale experiments.

$$U^{+} = U^{*} G_r^{1/2} P_r^{2/3} \tag{1}$$

$$X^{+} = X^{*} G_r^{-0.387} \tag{2}$$

$$Z^{+} = Z^{*} P_r^{1/4} \tag{3}$$

Where U^{*} is the dimensionless wind speed, X^{*} and Z^{*} are the dimensionless length of the horizontal direction and the vertical direction, respectively. G_r and P_r are Grashof and Prandtl number, respectively. The representative wind speed and the representative length are defined by;

$$U = \frac{g\beta\Delta\Theta}{\omega} \tag{4}$$

$$L = \left(\frac{\nu}{\omega}\right)^{\frac{1}{2}} \tag{5}$$

where g is the gravitational acceleration, β is the volumetric expansion coefficient, $\Delta\Theta$ is the maximum temperature difference of the surface temperature variation, ω is the angular velocity of earth's rotation and ν is the eddy diffusivity of momentum. Grashof number G_r and Prandtl number P_r are expressed by;

$$G_r = \frac{g\beta\Gamma L^4}{\nu^2} \tag{6}$$

$$P_r = \frac{\nu}{\alpha} \tag{7}$$

where Γ is the mean atmospheric temperature gradient and α is the eddy diffusivity of heat. The typical values of α , β etc. in this experiment and in the field are shown in Table 1. ω is used only for time adjustment of a day in the experiment. Equating both cases of experiment (taken as 1mm) and field of wind speed, horizontal length and vertical length by using equations 1, 2 and 3

respectively, the relation of the wind speed, horizontal length and vertical length of the experiment and the field are calculated as shown in Table 2 by using the values of Table 1. The similarity variables of U^+, X^+ and Z^+ in the experiment as well as the field are also shown in Table 2 which are reasonable and show that present water-tank experiment successfully simulated the air pollution mechanism of Kathmandu valley.

Table 1. Typical values of physical variables in the experiment and in the field.

	β [K^{-1}]	ν [m^2/s]	α [m^2/s]	ω [rad/s]	Γ [K/s]	$\Delta\Theta$ [K]	G_r	P_r
Experiment	2.07×10^{-4}	10^{-6}	1.43×10^{-7}	8.73×10^{-3}	100	5.6	2.63×10^{3}	6.99
Field	3.41×10^{-3}	10	10	7.27×10^{-5}	0.005	15	3.16×10^{4}	1

Table 2. Relation between experiment and field.

	Experiment	Field
Wind speed	1 [mm/s]	4.4 [m/s]
Horizontal length	1 [mm]	90 [m]
Vertical length	1 [mm]	56 [m]
U^+	0.22	0.10
X^+	0.22	0.25
Z^+	3.04	3.10

In consideration of above calculation in Table 2, a simple Kathmandu valley model is designed and constructed to analyze the winter air pollution dispersion mechanism. The horizontal length of valley is 150 mm in experiment which corresponds 13.5 km of the field (Kathmandu Valley) and 20 mm of the valley depth corresponds to the 1120 m high mountains of the field from ground surface of the valley. Thought X^+ and Z^+ are almost similar in the experiment as well as in the field, the wind speed for the field is found a little smaller than the one obtained by the similarity rule.

2.2 Experimental Set - Up

The set-up of our water-tank experiment is shown in Fig. 1. This set-up consists of three water-tanks. The middle tank (500 mm×400 mm×70 mm) filled with pure water was regarded as the atmospheric layer of Kathmandu valley. The water temperature in the top tank was kept at a constant while the water temperature in the bottom tank was changed with a constant period and amplitude in order to change the lower surface temperature of the middle water-tank which was assumed to be the ground surface of Kathmandu valley.

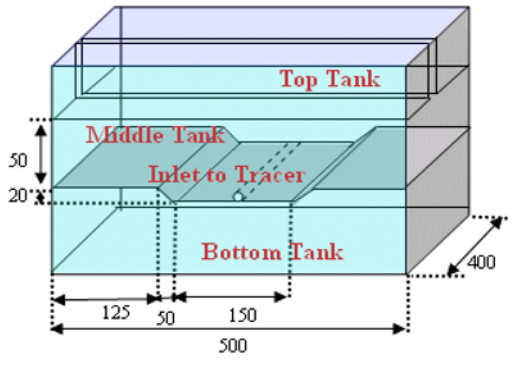

Fig. 1. Set-up of the water-tank experiment.

2.3 Experimental Method

The schematic flow diagram of the experiment is shown in Fig. 2. The water temperature of the top tank and the lower tank were kept at 40 ℃ and 35℃ respectively for 3 hours so that the thermal stratification with constant temperature gradient was formed in the middle tank as the initial condition of the experiment. A laser beam was focused at the central cross section of the middle tank by passing the laser beam through a slit provided at the top tank to take the images for measuring the temperature, velocity and mass dispersion with a CCD camera. From the start of the experiment, the bottom surface temperature of the middle water-tank was changed with the period of 12 minutes as shown in Fig. 3. The temperature pattern of the experiment resembles the 24 hours ground temperature variation pattern of Kathmandu Valley during February and 12 minutes experimental time corresponds to the local time of Kathmandu valley as also shown in Fig. 3. All the measurements of temperature, velocity and mass distribution were carried out in that condition.

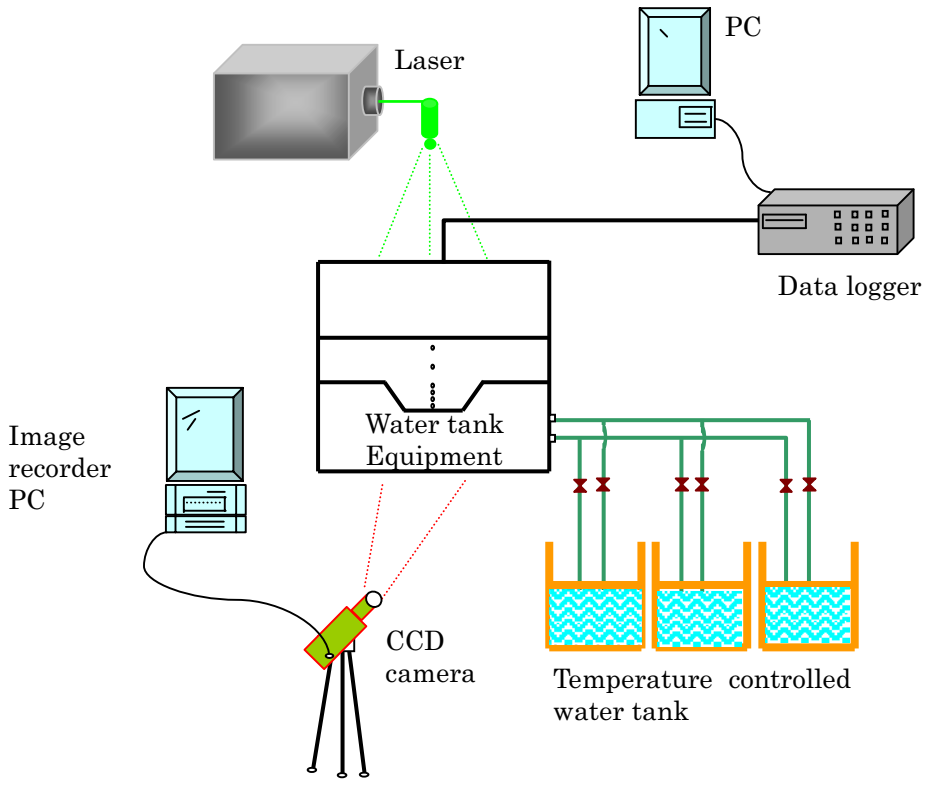

Fig. 2. Schematic flow diagram for temperature, flow field and mass dispersion measurement in water-tank experiment.

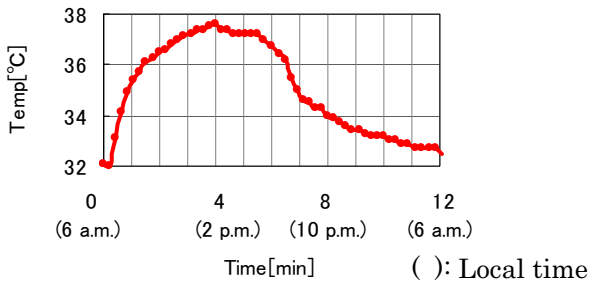

Fig. 3. Bottom surface temperature in the middle tank.

2.3.1 Measurement of Temperature

Thermocouples were used to measure the temperature in the middle tank at the height of 0 mm, 5 mm, 10 mm, 15 mm, 20 mm, 40 mm, 60 mm, top tank and the valley surface. The 20 mm height corresponds to the mountain height of Kathmandu valley. The temperature distribution of the entire valley region in the water-tank experiment was also visualized by using a thermo liquid crystal sheet. The thermo liquid crystal sheet having the same inner size and shape as that of the Kathmandu valley model was placed at the central cross section of the middle tank.

Several researchers (Dabibi and Gharib, 1991; Ozawa et al.,1992; Kimura et al.,1993) have used hue for converting the color information into the temperature but as the observation area in our water-tank experiment was wide and uniform illumination in the whole area was difficult, this method could not be adopted. Therefore, the temperatures of the entire region were determined by calibrating the RGB (red, green and blue colors) luminance intensity of each pixel from the entire image taken through a color CCD camera versus temperature (Kaga et al., 1999). The calibration of the thermo liquid crystal sheet was done from temperature 32 ℃ to 40 ℃ at the interval of 1 ℃. After the calibration, the images of the color change of thermo crystal sheet were digitalized every 1.5 seconds. A typical example of the luminance intensity of RGB at a certain pixel (i, j) versus calibration temperature is shown in Fig. 4.

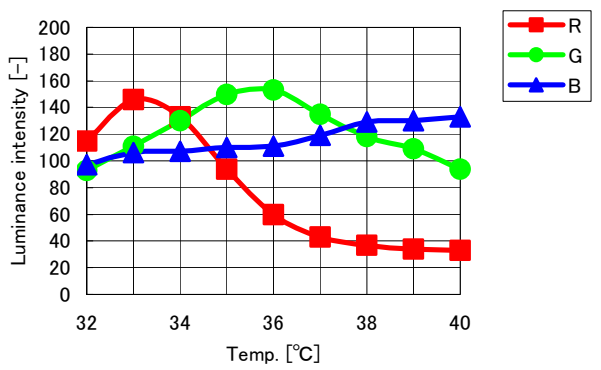

Fig. 4. Calibration of luminance intensity of RGB.

The luminance intensity of R and G possessed the same value at two different temperatures, and the slope of B was also very low. Therefore, the value of the temperature was designated to minimize the error value as E, defined by the following equation.

$$\{E(i,j,T)\}^2 = \{R(i,j) - R(i,j,T)\}^2 + \{G(i,j) - G(i,j,T)\}^2 + \{B(i,j) - B(i,j,T)\}^2 \quad (8)$$

Here, $R(i,j)$, $G(i,j)$, $B(i,j)$ are the luminance intensity of RGB in the experiment image at the pixel of (i,j), and $R(i,j,T)$, $G(i,j,T)$, $B(i,j,T)$ are the luminance intensity of RGB at temperature T in the calibration curve.

2.3.2 Measurement of Flow Field by PIV

Styrofoam was formed into fine particles by using an electric mixer and was suspended in water for 3 hours to select the particles having the same density as water. These fine particles were used as PIV tracers. These tracers were suspended homogeneously in the water in the middle tank. Six hundred frame images were taken up to 15 minutes with the interval of 1.5 seconds.

A Particle Image Velocimetry (PIV) method developed by the authors (Kaga et al., 1993) was used for the measurement of the flow field from visualized images. Generally, PIV analysis is done by finding the movement of the gray level pattern of a fixed shape of interrogation area (usually rectangular area) and it is very difficult to extract the velocity vector at the vicinity of inclined surface. But in our research, flow field along mountain slope is also important. Therefore, the image having the slope (Fig. 5(b)) was converted into rectangular image (Fig. 5(c)) and vector extraction

was done on the converted image (Fig. 5(d)). Later, the vectors were transformed back to their original image (Fig. 5(e)). This reverse transformation of the vector was performed by reversely transforming the coordinates of starting and terminal point of the vector expressed with converted coordinate to the original coordinate.

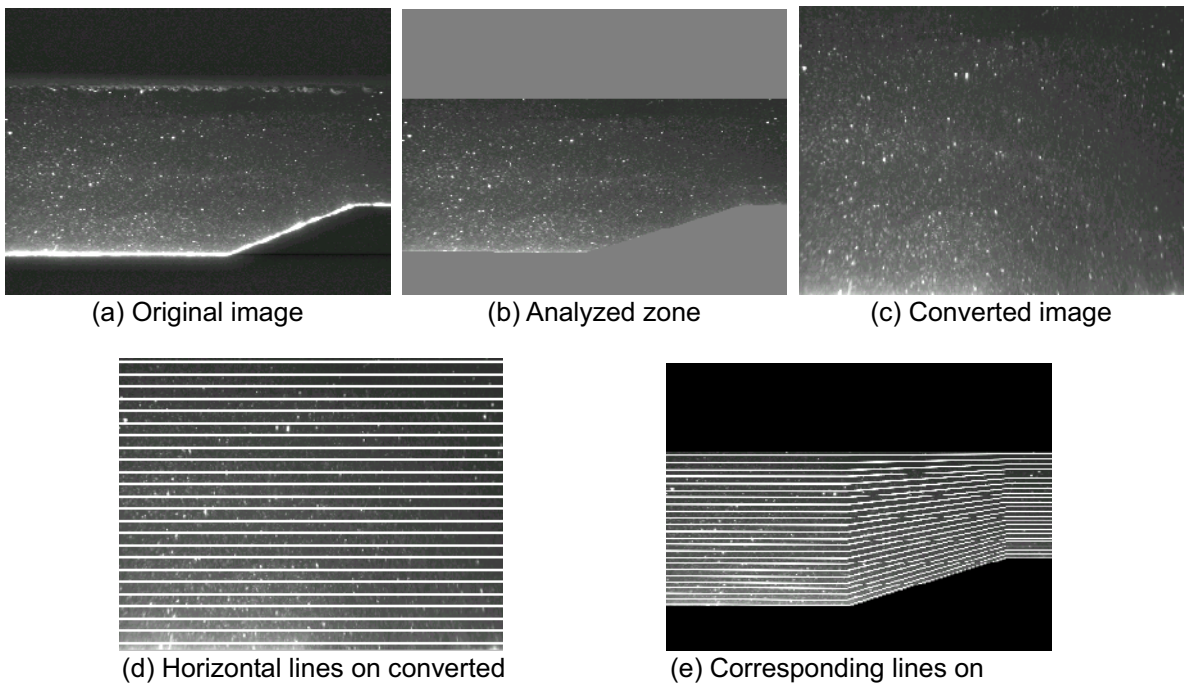

(a) Original image (b) Analyzed zone (c) Converted image

(d) Horizontal lines on converted image (e) Corresponding lines on original image

Fig. 5. Image conversion for PIV at the point near uneven surface.

The coordinate transformation of the analyzed zone from Fig. 6(a) to rectangular image 6(b) was done by the following equation.

$$Z^* = S\left(\frac{Z - Z_G}{H - Z_G}\right)^m \tag{9}$$

Where Z is the vertical coordinate, Z^* is the transformed vertical coordinate, Z_G is the bottom height of the middle tank before transformation, H is the top height of the analyzed region before transformation and S is the top height of the analyzed region after transformation. Through the coordinate transformation, $Z=Z_G$ was transformed to $Z^*=0$ and $Z=H$ was transformed to $Z^*=S$. Here, the value of m was taken as 0.9 to enlarge the lower analyzed region in comparison with the upper region [Figs. 5(d, e)].

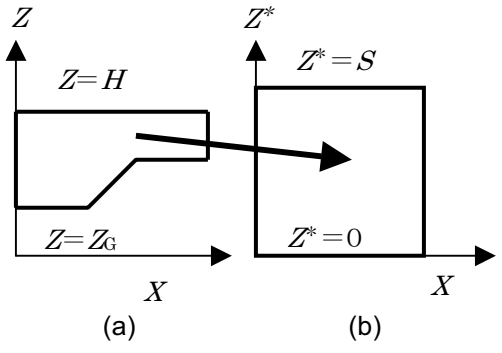

Fig. 6. Coordinate for image conversion.

2.3.3 Measurement of Mass Dispersion Characteristics

The fluorescence dye (Uranine: 30 mg/ℓ) was used as tracers for the experiment. For the calibration of the tracer concentration, Uranine solution up to 10 ml, made by adding 2 ml at each step was mixed homogeneously with the water contained in the middle tank and the images were taken at all steps. Calibration of RGB was done from the images taken during the addition of 2 ml of Uranine solution at each step. Calculated luminance intensity of RGB in the whole image suggested that R and B were almost negligible and G demonstrated almost the linear characteristics. Therefore, luminance intensity of G was used as the mass concentration.

The tracers were injected uniformly at midnight (3 a.m.) during the experiment from a small tube kept on the center of the bottom of the middle tank. The tracers were considered as the pollutant in the valley emitted at 3 a.m. Similarly, the tracers were injected at 3 p.m. to compare the mass dispersion characteristics in the valley between daytime and nighttime. The injected tracer puff moved by flow and diffused as the time proceeded. The standard deviation of the concentration distribution around the centroid was calculated to quantify the extent of diffusion of the puff. The centroid coordinate $(\bar{x}, \bar{y})$ of the puff was calculated by

$$(\bar{x}, \bar{y}) = \left(\frac{\sum x(i,j)c(i,j)}{\sum c(i,j)}, \frac{\sum y(i,j)c(i,j)}{\sum c(i,j)} \right). \tag{10}$$

The standard deviation of concentration distribution was calculated by

$$\sigma = \sqrt{\frac{\sum \left\{ \left(x(i,j) - \bar{x} \right)^2 + \left(y(i,j) - \bar{y} \right)^2 \right\} c(i,j)}{\sum c(i,j)}}, \tag{11}$$

where $c(i, j)$, $x(i, j)$ and $y(i, j)$ are the tracer concentration, x and y coordinate of each pixel (i, j) respectively.

3. Results and Discussions

In describing the experimental results, local time is used instead of the experiment time in order to make easy understanding of the field phenomenon.

3.1 Temperature

The changes in temperature measured by thermocouples are shown in Fig. 7. The amplitude of temperature variation on the surface of the middle tank was 5.5 ℃ in the experiment which corresponds to 15 ℃ field temperature of Kathmandu valley. This temperature gives the maximum temperature difference of Kathmandu valley during winter season. The effect of the change of temperature on the surface was seen up to 20 mm vertical height which was equivalent to 1120 m in the field. Figure 7 showed the formation of the inversion layer taking place from 9 p.m. to 9 a.m. of the next day.

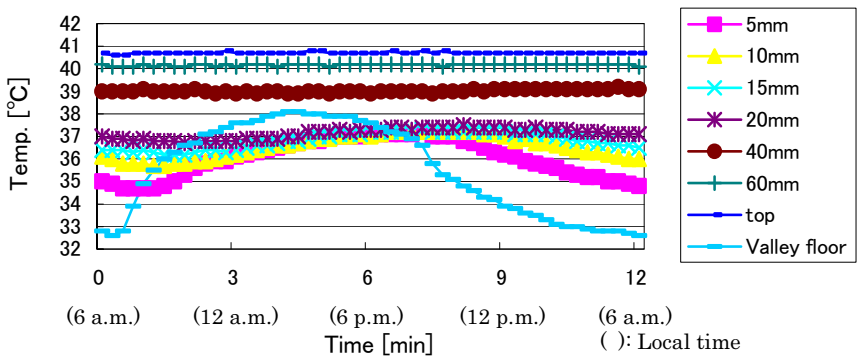

Fig. 7. Vertical distribution of temperature in water-tank.

The temperature distribution of the entire region of middle tank measured with the thermo liquid crystal sheet is shown in Fig. 8. Temperature contour lines seem almost parallel except for the vicinity of the ground surface. The temperature contour lines were found dense near the ground surface at nighttime while the temperature stratification became weak in the daytime. The temperature at the bottom layer was found lower than the initial condition from 10 p.m. to 8 a.m. of the next day in the images. The formation of the inversion layer in the nighttime was also confirmed by Shrestha et al. (2002a) by measuring the vertical distribution of temperature at Mt. Raniban, Kathmandu (altitude of 60 m, 220 m and 540 m above the ground surface of the Institute of Engineering, Pulchowk, Tribhuvan University). Shrestha et al. (2002b) got the similar temperature distribution by numerical calculation of the water-tank. The inversion layer phenomenon was also realized in the present experiment.

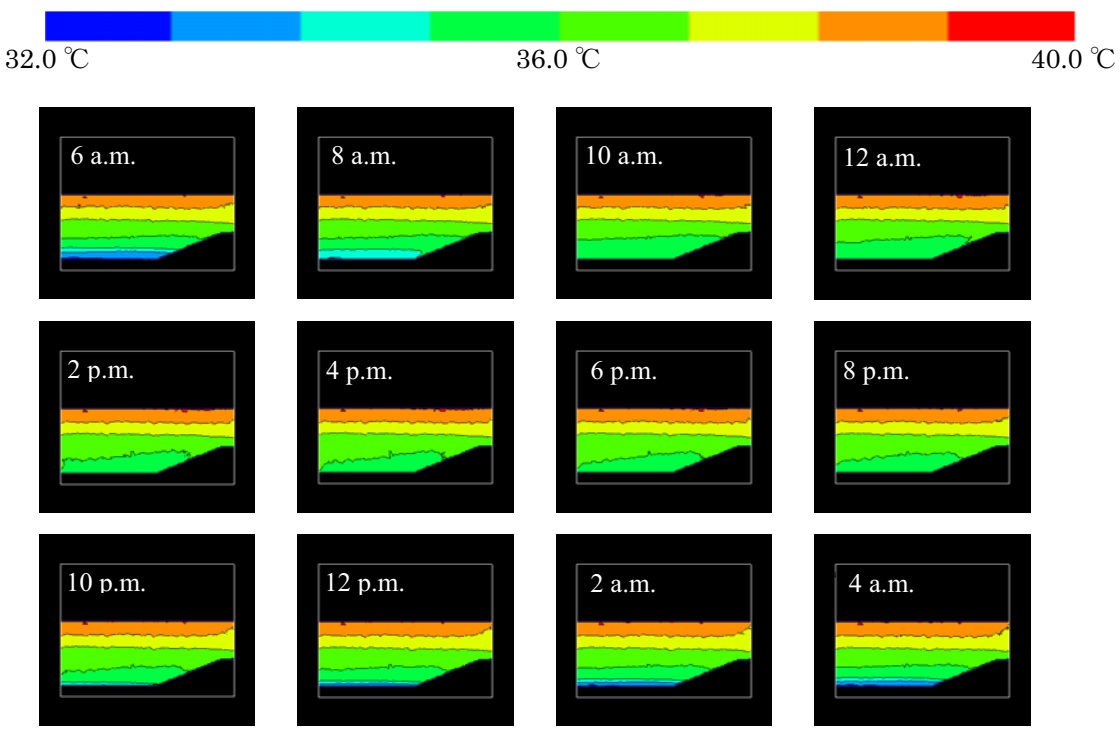

Fig. 8. Temperature distribution calculated from the thermo liquid crystal sheet.

3.2 Flow Field

Results of the velocity distribution measurements are shown in Fig. 9. After the temperature inversion (stable layer) was generated, the flow field was quite calm until 6 a.m. The field near the ground surface started to flow after the temperature inversion disappeared at 8 a.m. High value of updraft wind and Bernard convection occurred from 10 a.m. to 2 p.m. The maximum updraft wind obtained in the experiment was 1.5 mm/s at 2 p.m. which corresponds to 6.6 m/s in the field according to the similarity rule. The observation data obtained from Department of Hydrology and Meteorology (DHM), Airport Section, Kathmandu, indicated that the daily maximum wind velocity in the daytime was 4 m/s during winter season. Updraft wind was seen clearly in the daytime. Such an updraft wind system is quite similar to the one suggested by Barry (1981). The flow field was observed almost calm from 6 p.m. The wind velocity measured at DHM also showed calm wind in the nighttime during the winter season. Downdraft wind was observed at the slope of the valley from 8 p.m. to 6 a.m. in the next day.

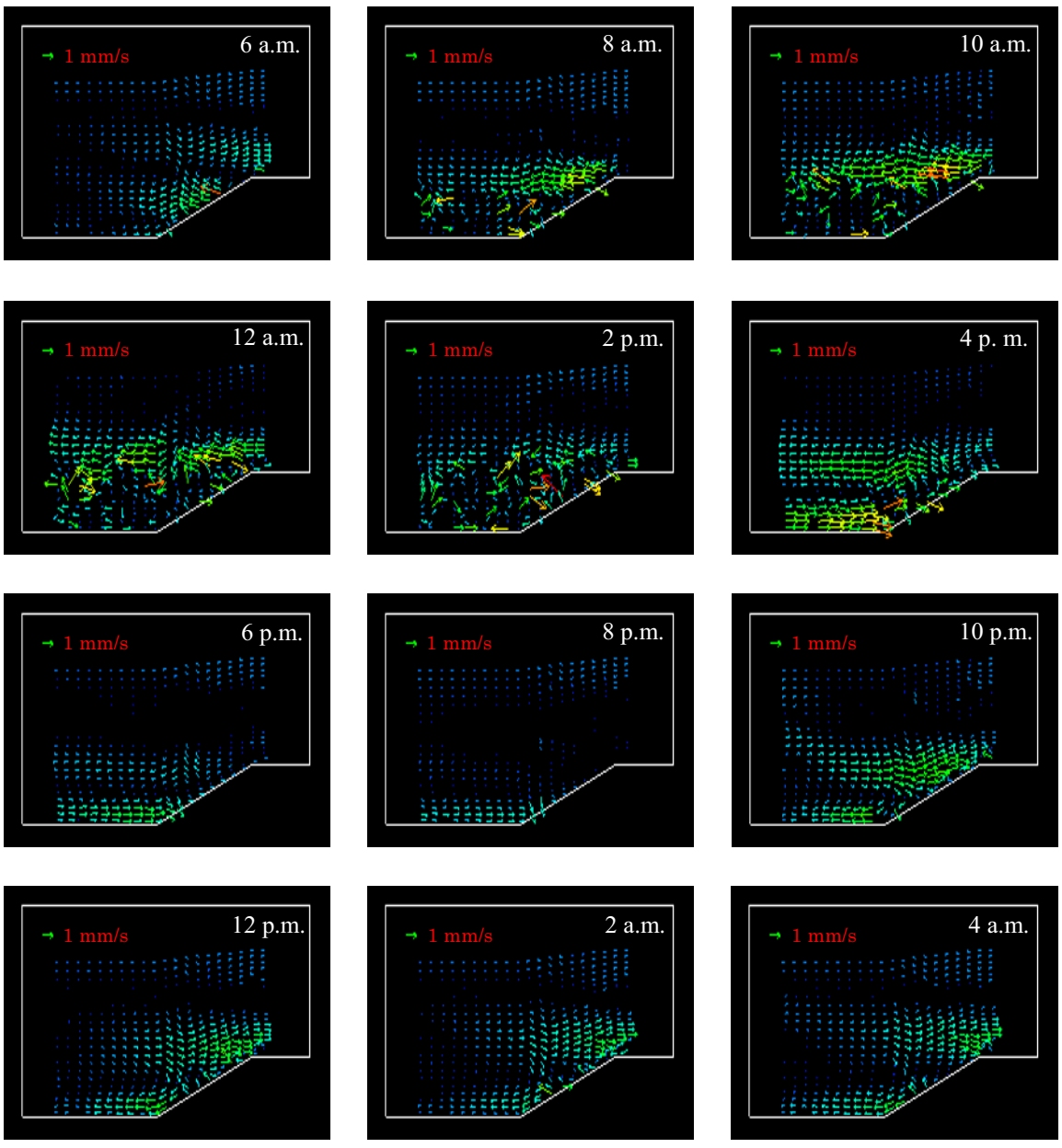

Fig. 9. Flow field extracted from visualized images.

3.3 Mass Dispersion Characteristics

The dispersion of tracers emitted in the nighttime and daytime are shown in Fig. 10 and Fig. 11 respectively. The tracers emitted at 3 a.m. did not disperse even after 2 hours of emission. The dispersion gradually took place at 6 a.m. Such phenomenon occurred due to the very calm flow field and the formation of inversion layer in the nighttime. Updraft wind started to occur and the rate of dispersion speeded up corresponding to the high temperature in the daytime after 8 a.m. as shown in Fig. 10. On the other hand, Fig. 11 shows that the tracers emitted at 3 a.m. immediately rose up and dispersed around the vicinity of the emission within an hour.

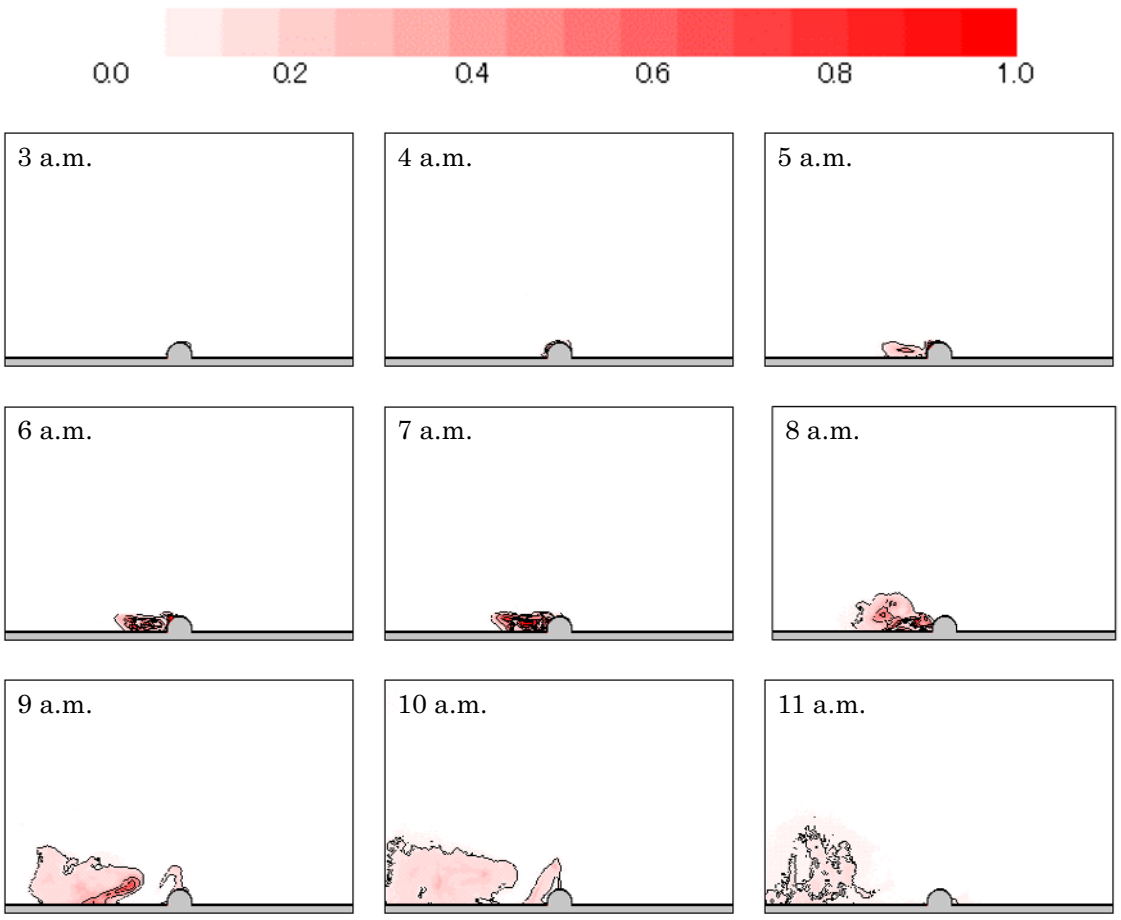

Fig. 10. Mass dispersion of the tracer emitted at 3 a.m.

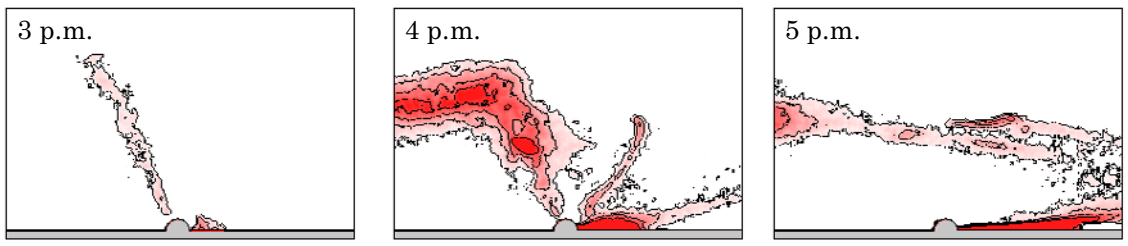

Fig. 11. Mass dispersion of the tracer emitted at 3 p.m.

The time change of the standard deviation of the distribution of tracer concentration after the emission of tracers at 3 a.m. and 3 p.m. are shown in Fig. 12. The graph suggested that the dispersion in the nighttime (3 a.m.) was extremely suppressed when compared with daytime (3 p.m.). The rate of dispersion in the nighttime was very slow and remained suppressed till approximately 5 hours after the emission of tracer. The mass transport coefficient was small until that time when the temperature was low in the water-tank experiment. The rate of dispersion in the daytime was found very high in comparison with that in the nighttime. When standard deviation of concentration distribution was compared after 2 hours of emission, daytime dispersion was found to be approximately 10 times faster than that in the nighttime.

The results obtained from the water-tank experiment can be related with the atmospheric phenomenon of Kathmandu valley. The dispersion of pollutant becomes small during the night as it gets cold. If the pollutant sources are present in the valley, the pollutant will remain in the vicinity of

the sources for a long time due to the formation of the inversion layer, the very weak flow and downdraft wind. The presence of many sources of pollutants may affect the entire area severely, resulting in high pollutant levels in the valley. When the Kathmandu valley gets warm by sun rays, updraft wind and Bernard convection cause higher dispersion rate in the daytime, resulting low pollutant levels in the daytime.

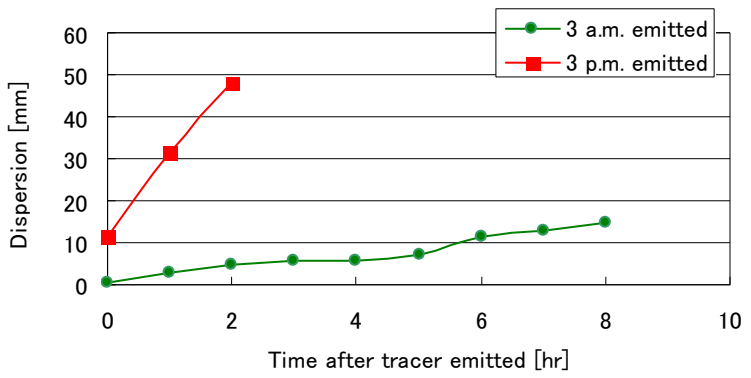

Fig. 12. The dispersion after emission of tracers.

We measured the NO_2 and TSP at the Institute of Engineering in Kathmandu during the winter season which showed higher pollutant concentration from night to early morning, rather than in the daytime (Shrestha et al. 2002a). During that time, large numbers of brick kilts were under operation even in the nighttime. Due to the low rate of diffusion of pollutant, downdrift flow and the formation of the temperature inversion, anthropogenic pollutant emitted in the nighttime might accumulate in the Kathmandu valley causing high concentration of pollutant in the early morning. The high pollutant concentration of the Kathmandu valley during winter season was simulated by water-tank experiment and the results are believed to elucidate the field measurements qualitatively. The mechanism suggested above by the present water-tank experiment logically supports the reason of high pollutant level in the Kathmandu valley during winter season in the nighttime and early morning.

4. Conclusion

The high air pollution mechanism in the Kathmandu valley in winter was simulated by a water-tank experiment and quantitatively analyzed by visualized images. The formation of temperature inversion was attained in the water-tank. The flow field was measured by a PIV method. Updraft wind and Bernard convection occurred from 8 a.m. to 2 p.m. Downdraft wind and inversion layer occurred from 8 p.m. to 6 a.m. in the next day. Pollutant dispersion in the nighttime is found approximately 10 times weaker than that in the daytime. This phenomenon and anthropogenic emissions may cause the cyclic high air pollution in the valley from night to early morning. Brick factories, poorly maintained vehicles etc. may be considered as the source of anthropogenic pollutants within the valley. Therefore, it is suggested restricting such anthropogenic pollutants to improve the air quality in the Kathmandu valley. The improvement of fuel quality used in vehicles, domestic heating and cooking are also important factors to reduce the pollutants.

The methods used in the analysis of temperature, flow field and concentration in water-tank experiments are helpful to understand the air pollution dispersion mechanism influenced by the natural convection. A similarity rule developed for land and sea breeze was used in this research but detail study of the similarity rule for the valley model is required for future study.

References

Barry, R.G., Mountain weather and Climate, (1981), 313, Methuen, London.
Dabiri, D. and Gharib, M., Digital particle image thermometry, The method and implementation, Experiments in Fluids, 11 (1991), 77-86.
Kaga, A., Inoue, Y. and Yamaguchi, K., Pattern Tracking Algorithms Using Successive Abandonment, J. of Flow Visualization and Image Processing, 1 (1993), 283-296.
Kaga, A., Yamaguchi, K., Inoue, Y. and Kondo, A., A laboratory experiment on land and sea breeze through PIV, ASME & JASME Fluids Eng. Conf. (South Carolina), FED, 218 (1995), 139-143.
Kaga, A., Tani, A., Inoue, Y., Abe, T. and Yamaguchi, K., Experiment of water-tank model for displacement ventilation using image processing, J. Visualization Soc. Japan, 19, Suppl. 2 (1999), 107-110 (in Japanese).
Kimura, I., Kuroe, Y. and Ozawa, M., Application of neural networks to quantitative flow visualization, Journal of Flow Visualization and Image Processing, 1 (1993), 261-269.
Kondo, A., Shrestha, M. L., Kaga, A., and Inoue, Y., Comparison of field observation with water-tank experiment on air pollution concentration in Kathmandu valley, Air Pollution X (Segovia, Spain) (2002),493-502, WIT press.
Heping, L., Boyin, Z., Jianguo S., and Andrew Y. S. C., A laboratory simulation of plume dispersion in stratified atmospheres over complex terrain, J. of Wind Engg. and Industrial Aerodynamics, 89 (2001), 1-15.
Matsumoto, S., Ueda, H. and Ozoe, H., A Laboratory Experiment on the Dynamics of the Land and Sea Breeze, J. of Atmospheric Science, 40 (1983), 1228-1240.
Ohba, R., Kakishima , S. and Ito S., Water-tank experiment of gas diffusion from a stack in stably and unstably stratified layers under calm conditions, Atmospheric Environment, 25-10 (1991), 2063-2076.
Ozawa.m., Mullet, U., Kimura, I. and Takamori, T., Flow and temperature measurement of natural convection in a hele-show cell using a thermo-sensitive liquid- crystal tracer, Experiments in Fluids, 12 (1992), 213-222.
Park, O.H., Seo, S. J. and Lee, S. H., Laboratory simulation of vertical plume dispersion within a convective boundary layer, Boundary Layer Meteorology, 99 (2001), 159-169.
Shrestha, M. L., Kaga, A., Kondo, A. and Inoue, Y., Diurnal Air Pollution Variation of Kathmandu Valley, Proceedings of the 42th Symposium on Japan Society for Atmospheric Environment (Kyusyu, Japan) (2001), 521.
Shrestha, M. L., Kaga, A., Kondo, A., Inoue, Y., and Sapkota, B., Diurnal Variation of Air Pollution Concentration during Winter in Kathmandu Valley, Air Pollution X (Segovia, Spain) (2002a), 653-662, WIT press.
Shrestha, M. L., Kaga, A., Kondo, A. and Inoue, Y., Winter air pollution Mechanism of Kathmandu valley by Water-tank experiment, 10th international symposium on flow visualization (Kyoto, Japan), August 26-29 (2002b), 64.
Ueda, H., Effects of External Parameters on the Flow Field in the Coastal Region - A Linear Model, J. of Appl. Meteor., 22 (1983), 312-321.

Author Profile

Manohar Lal Shrestha: He graduated his B. E. degree in Mechanical Engineering from Aligarh Muslim University, India in 1991 and worked at Toyota Nepal (United Traders Syndicate Pvt. Ltd., Nepal) as a Service Manager. He joined the R & D section of Fujikin Incorporated, Japan, in 1992 as an engineer. He got his M.E. degree in Environmental Engineering from graduate school of engineering, Osaka University, in 2002. Currently, he is a Ph. D. candidate in Osaka University and his research interests are atmospheric pollution mechanism, air flow measurement using flow visualization and image processing.

Kaga Akikazu: He received his B. E. degree in 1969, M. E. in 1971 in Mechanical Engineering, and his D. E. degree in 1985 in Environmental Engineering from Osaka University. He has been working in Osaka University from 1971 as an assistant professor, from 1988 as an associate professor and from 2000 as a professor. His current research interests are airflow measurement using flow visualization and image processing, and the analysis and management of air pollution problems in Asian cities.

Akira Kondo: He received his B. E. degree in 1982, and M. E. degree in 1984 and his D. E. degree in 1999 in Environmental Engineering from Osaka University. He worked in Matsushita Industrial Co. till 1989. After that, he worked as an assistant professor in the Department of Environmental Engineering in Osaka University. Currently, he is working as an associate professor and his research interests are numerical simulation model of atmospheric boundary layer and environment management in South-East Asia.

Yoshio Inoue: He received his B. E. degree in 1973 in mechanical engineering from Osaka Institute of Technology and his D. E. degree in 1999 in Environmental Engineering from Osaka University. He has been working in Osaka University from 1971 as a technician and as an assistant professor from 1988. His current research interests are airflow measurement using flow visualization and image processing, and automatic recognition of aerosol particles such as asbestos fibers and allergic pollens from microscopic image of specimen using image processing.

Masahiko Sugisawa: He graduated his B.E. degree in Environmental Engineering from Osaka University in 2002 and is currently a master student in the same University and his research interests are atmospheric pollution mechanism, air flow measurement using flow visualization and image processing.

Balkrishana Sapkota: He received his M. Sc. (Physics) from Tribhuvan University, Nepal in 1980, M. Tech. (Hydrology) from University of Roorkee, India in 1984 and got the Ph. D. from same University in 1988. He joined Trichandra College, Tribhuvan University (T.U.) as an Assistant Lecturer in 1981. He moved to Institute of Engineering, T.U. to work as a Lecturer in 1988. Currently, he is working as a associate professor at Institute of Engineering, Nepal. His research contributions include measurement/analysis of Air pollutant, Noise Pollution and development of Global Circuit Model to study the variation of atmospheric electrical parameters due to variation in air pollutant.